A comparative Study of the Effectiveness of Empirical Potentials for Molecular Dynamics Simulations of Borosilicate Glasses

Manzila Islam Tuheen, Lu Deng, Jincheng Du*

Department of Materials Science and Engineering, University of North Texas, Denton, Texas

(*Corresponding author. Email: du@unt.edu)

Abstract

Despite their practical importance, atomistic modeling of B_2O_3 containing glasses have been challenging due to the lack of reliable empirical potentials. Fortunately, a few recent developments have shown promises to simulate these glasses where the boron coordination has complex and non-linear dependence on glass composition. This work aims to provide an evaluation of the effectiveness of three recently developed potentials by a systematic study of a series (~20) of sodium borosilicate glasses with constant K (ratio of $[SiO_2]/[B_2O_3]$) =2 and varying R (ratio of $[Na_2O]/[B_2O_3]$ ranging from 0.1 to 4) values and several sodium boroaluminosilicate glasses. A comparative assessment was established on the basis of the short- and medium-range structure features, such as boron N_4 values, total correlation functions, bond angle distribution, oxygen speciation, and mechanical properties using experimental or well-established models as criteria. This work provides insights on the choices of empirical potentials for MD simulations of borosilicate glasses and gives directions of future potential development and refining.

Key words: molecular dynamics, empirical potentials, borosilicate glass, mechanical properties, potential evaluation

1. Introduction

Since the earliest of its development, borosilicate glass has been a significant member of the glass world and applied in diverse fields of scientific, industrial and technological domains. Along with the traditional usage of these glasses as sealing glass, heat and chemical resistant glass containers, optical components and fiber glasses[1]–[4], borosilicate glasses have attracted immense attention from the glass scientists due to its potential importance in immobilization nuclear waste and biomedical applications [5]–[9]. Pure B_2O_3 glass, if broken down to the simplest of the structures, has BO_3 triangles as its building block and often contains larger

structure units such as boroxyl rings. The structure of borate and more complex compositions such as borosilicate and boroaluminosilicate glass is much more complicated due to the presence of composition dependent boron coordination changes and competition for oxygen from modifier oxides among the glass formers [10]. Borate or borosilicate glasses demonstrate a non-linear composition to property relationship and this phenomenon is known as boron anomaly [11]–[13]. In alkali borosilicate glass, the alkali ion can either break the Si-O-Si bond and generate non-bridging oxygen or it can convert $^{[3]}$B or three coordinated boron to $^{[4]}$B or four-coordinated boron by playing the role of charge compensation. This conversion from three to four coordinated boron as the origin of boron anomaly was first confirmed by ^{11}B solid state NMR experiment [14]–[16]. As a consequence of the boron anomaly, the structure and properties such as density, glass transition temperature, elastic moduli of a typical alkali borate and borosilicate glasses show non-linear relations to the molar ratio R=[Na_2O]/[B_2O_3]. The fraction of four-fold coordinated B, or commonly known as the N_4 value, first increases linearly and then reaches a maximum at R_{max}. This maxima R_{max} is around 0.3 for alkali borate glasses but it also depends on the type of modifier oxide and existence of other glass former oxides, such as the molar ratio K = [SiO_2]/[B_2O_3] in borosilicate glasses. Therefore, first proposed by Yun and Bray [17] and then refined by Dell, Bray and Xiao [14], named as the DBX model, to predict the fraction of four-coordinated boron (N_4) for wide variety of glass compositions using the input of R and K values based on NMR studies of a wide range of sodium borosilicate glass compositions [14]. There are additional factors to be considered in case of sodium boroaluminosilicate glasses because both glass formers, boron and aluminum compete for oxygen and alkali ions for charge compensation which in turns affects the N_4 yields [18]. In these glasses, sodium oxide first chooses to charge compensate aluminum and then the rest of the Na^{1+} yields a decreased amount of N_4 compared to that of sodium borosilicate compositions with same ([Na_2O]-[Al_2O_3])/[B_2O_3] ratio and K values. In order to interpret the structures and properties of sodium boroaluminosilicate glasses as functions of R and K, Du and Stebbins [19] substituted these parameters by R'= [Na_2O]/([B_2O_3]+ [Al_2O_3]) and K'= [SiO_2]/([B_2O_3]+ [Al_2O_3]). This model demands another criterion that the concentration of sodium oxide needs to be more than that of aluminum oxide since [Na_2O]-[Al_2O_3] will be taking part in $^{[3]}$B to $^{[4]}$B conversion and generating non-bridging oxygen (NBO) for silicon tetrahedron.

Atomistic level simulations have been a powerful tool in the study of glasses and many other non-crystalline materials. Molecular dynamics (MD) simulations, in particular, have been highly valuable in elucidating the structure and the structure-property analysis of these materials. The choice of an appropriate empirical potential set is the key to the success of MD simulations. Despite the growing interest for boron oxide containing glasses, the number of empirical potentials developed for these systems has remained very few. This is mainly because of the simultaneous presence of tri- and tetra-coordinated boron that are composition and thermal history dependent. For example, the presence of other glass formers such as silicon and aluminum causes mixed glass former effect due to their mutual interactions. The complex nature of the system and the difficulty in describing the boron anomaly makes it extremely challenging to obtain reliable empirical potentials hence to simulate boron containing glasses. Several empirical potentials have been developed in the literature, adopting different approaches to address the boron coordination changes. Early MD simulations of borosilicate glasses used the Born-Mayer-Huggins (BMH) pair potentials [20]. Even though this particular set of potentials resulted in reasonable atomic structures but the mechanical properties showed large deviation from experiments [21]. Again, BMH potential uses integer charges of the ions which did not properly describe the partial covalency of the silicate network. Appropriate modelling of such systems then demanded potential sets with variable parameters to better describe the changing boron environment with glass compositions. Takada et al. [22], [23] proposed a set potential where boron coordination regulates the interaction between boron and oxygen. Another set of potentials developed by Huang and Kieffer [24], [25] introduced three-body interaction and atomic charge transfer depending on the local environment of boron. But this potential set only include B_2O_3 and the complicated potential form demands high computational expense. Inoue et al.[26] proposed a set partial charge pairwise potential which is able to reproduce boron anomaly in accordance with the composition change. Kieu et al [27] introduced composition dependent charge values for sodium borosilicate glasses which well reproduces the structure and mechanical properties. To this potential set, Deng and Du [28] added aluminum related parameters to be able to simulate alkali boroaluminosilicate glasses. Deng and Du [29] proposed a set of potentials based on Teter parameterization which involves compositional dependency of boron related parameters. Since composition dependent atomic charges and parameters diminishes the transferability of these potentials, simple formulations of the potential set was

proposed by Wang et al. [30] based on Guillot-Sator parameterizations for oxides and minerals [31]. This potential set has fixed parameters but introduced cation-cation interactions. A few recent studies have provided a comparison of MD simulations of borosilicate glasses using some of these potentials but a systematic comparison of a wide compositions range is still not available. Several polarizable potentials have also been used where the anion polarizability was described either by the shell model [32] or the polarizable ion model (PIM)[33], [34]. Fortino et al. [35] assessed the interatomic potential sets developed by Deng and Du [29] and Wang et al. [30] along with shell model based potential developed by Stevensson et al. [32] in MD simulations of a series of borosilicate glasses $25Na_2O\text{-}xB_2O_3(75\text{-}x)\text{-}75SiO_2$ (x=0-75 mol%) using DFT-GIPAW calculations. The calculated ^{11}B, ^{29}Si and ^{23}Na NMR spectra were used as a means to evaluate the effectiveness of the potentials in reproducing the glass structures. It was found that the two rigid ion potentials can both describe the B^3/B^4 partitioning well in the systems but the polarizable potential better described the second coordination shell of Si and the Si-O-T (T=B,Si) bond angles hence give better agreement of the calculated ^{29}Si MAS NMR spectra as compared to experiments [35]. Lee et al. [36] established a comparative study of the potential sets of Deng and Du [29] and Wang et al.[30] in analyzing the structure and elastic properties of a pair of commercial borosilicate glasses denoted as Boro33 and N-BK7. Neutron structure factors calculated from MD configurations were compared with the experimental data and short and medium range structures of the two glasses from the two sets of penitential were evaluated. It concluded that the Wang et al potential provided better prediction of short-range structures while Deng and Du potential provide better medium range structure descriptions. The focus of the two compositions might limit the evaluation of the potentials. Even though these studies have provided insights into the compatibility of these potentials sets in modeling borosilicate glasses via MD simulations, a comprehensive and systematic analysis of these potential sets is still not available in the literature.

In this work, we aim to establish a comparative study of three widely used boron containing empirical potentials: which are proposed by Deng and Du [29], Kieu et al. [27] and Wang et al. [30], respectively. Different in characteristics and formulations, all three of these potential sets show promising aspects to be applied in MD simulations of borosilicate and boroaluminosilicate glasses. The goal of this work is to provide a systematic evaluation of the three potentials for their application in simulations of borosilicate and boroaluminosilicate glass compositions with

wide range of R values. This paper is arranged in the way to first provide brief introductions of the potentials sets, methodology of MD simulations for glass structure generations. The results section comprises of the findings from MD simulations using three of these potentials sets for ternary and quaternary boron containing glass systems. Lastly, prospects of these potential sets are discussed and final conclusions are made.

2. Simulation Details

2.1 Empirical potentials for borosilicate glasses

The present comparative analysis of the effectiveness of empirical potentials for MD simulations of borosilicate and boroaluminosilciate glasses includes three sets of boron potentials recently developed by Kieu et al. [27] (hereafter referred as Kieu potential), Wang et al. [30] (hereafter referred as Bauchy potential), and Deng and Du [29] (hereafter referred as Du potential), respectively. All of the three sets of potentials were developed aiming to perform MD simulations of borosilicate glasses. There are similarities as well as differences in their characteristics and approaches which brings about the variations in results obtained from MD simulations in terms of structural characteristics, mechanical properties and so on. All of the three potentials are pair potential in nature and there are no three body terms. They have the same form combining short-range Buckingham term and a long-range Coulomb term which can be expressed by the following expression:

$$V(r_{ij}) = \frac{Z_i Z_j e^2}{4\pi\varepsilon_o r_{ij}} + A_{ij}\exp(-r_{ij}/\rho_{ij}) - C_{ij}/r_{ij}^6 \quad (1)$$

where, r_{ij} represents the interaction distance between atom *i* and *j*; A, ρ, C describe different parameters for the Buckingham term. The long-range Columbic interaction takes partial charges of the ions into account to better describe the partial covalence and iconicity of the chemical nature of the bonds present in the system. Table 1 compared the oxygen-oxygen and cation-oxygen potential parameters while Table 2 listed the adopted atomic charges. Detailed of the composition dependent parameters and charges are discussed in the following sections. Cation-cation potential parameters that were used in the Kieu and Bauchy potentials were not listed but can be found in the original paper [29], [27]. No cation-cation interactions were used in the Du potential. Here we provide a brief summary of the three potentials.

Kieu et al. initiated an effort to develop reliable boron potentials for the simulations of sodium borosilicate glasses that are target glass systems for nuclear waste disposal [27]. Built up the partial charge pairwise potential developed by Guillot and Sator (GS potential) for silicate glasses and minerals for wide range of compositions in the geoscience community [31], [37], [38], Kieu et al proposed a novel composition dependent approach to address the composition dependent boron coordination in borosilicate glass [27]. The key assumptions include (1) the atomic charges depend on the ratio of $B^{[3]}$ and $B^{[4]}$, namely f_{B3} and f_{B4}, respectively, and (2) the short range B-O interaction should vary with the two boron coordination ratio. By developing analytical expressions for both terms based on the DBX model of boron coordination change with composition, the potential contains composition-dependent variable charges and A parameters for Buckingham term of the B-O interactions. It further assumes that the charge ratio of three- to four-coordinated boron (q_{B4}/q_{B3}) is a constant value of 1.14 and the charge ratios of each of these species to the partial charge of oxygen, q_{B3}/q_o and q_{B4}/q_o, remain constant of -1.5 and -1.71, respectively. Based on these rules, the expressions to calculate the average charge of B and the partial ionic charges of other species were developed. Furthermore, this potential adopted the variation of A_{ij} parameter for B-O interaction as a function of the chemical composition with connection to the DBX model. Additional terms of the cation-cation interactions were included to ensure the composition dependent boron coordination changes and to keep the basic structural features of the silicate glasses. Alumina is a common intermediate in borosilicate glasses but was not included in the original potential development. Later on Deng and Du [28] extended the potential to include alumina related parameters based on the coordination changes from NMR by Du and Stebbins[39] to enable the potential set to simulate sodium boroaluminosilicate glass systems. Both potentials will be used in the current work.

Another attempt of obtaining boron oxide potentials by Wang et al. [30] also adopted the GS potential framework [31] as the Kieu potential did [27]. The Bauchy potential was developed using simple formulations and constant parameters such as fixed partial charges of the ions with the aim to improve transferability and decrease the number of fitting parameters [30] pair potential parameters. The potential adopted partial charge of the GS potential in which the ionic charge of O is -0.945 while the charges of other cations, including B, are scaled according to their formal charges, e.g. the charge of Si, B and Na are 1.89, 1.4175 and 0.4725, respectively. A comparison of the charges used in the three potential set is listed in Table 2. Following the Kieu

potential [27], this potential continued the usage of B-B and B-Si cation-cation short range interactions. The potential were parameterized and validated on a series of sodium calcium borosilicate glasses [30]. The B-Si pair potential parameters were adopted from the Kieu potential set [27] while the B-O interaction parameters were adjusted to reproduce experimental boron coordinated in the quaternary borosilicate glass system. Subsequently, the B-B parameters were adjusted to be able to reproduce the density of the glass system.

Table 1 Buckingham potential parameters for Du [29], Kieu [27] [28]and Bauchy [30] potential sets

	Du [29]			Kieu [27] [28]			Bauchy [30]		
	A_{ij} (eV)	ρ_{ij} (Å)	C_{ij} (eV.Å^6)	A_{ij} (eV)	ρ_{ij} (Å)	C_{ij} (eV.Å^6)	A_{ij} (eV)	ρ_{ij} (Å)	C_{ij} (eV.Å^6)
B-O	Composition dependent			Composition dependent			206941.81	0.124	35.0018
Si-O	13702.9050	0.193817	54.681	45296.72	0.161	46.1395	50306.10	0.161	46.2978
Al-O	12201.4170	0.195628	31.997	28287.00	0.172	34.7600	28538.42	0.172	34.5778
Na-O	4383.7555	0.243838	30.700	120360.22	0.17	0	120303.80	0.17	0.0
O-O	2029.2204	0.343645	192.58	9027.03	0.265	85.0321	9022.79	0.265	85.0921
B-B	-	-	-	121.10	0.35	0.0	484.0	0.35	0.0
Si-B	-	-	-	337.70	0.29	0.0	337.7	0.29	0.0
Si-Si	-	-	-	834.4	0.29	0.0	-	-	-
Al-Al	-	-	-	351.94	0.360	0.0	-	-	-
Al-Si	-	-	-	646.67	0.120	0.0	-	-	-
Al-B	-	-	-	137.58	0.479	0.0	-	-	-
Al-Na	-	-	-	351.94	0.360	0.0	-	-	-

Table 2 Partial atomic charges of elements for the Du [29], Kieu [27][28] and Bauchy [30] potential sets

Element	Du [29]	Kieu [27][28]	Bauchy [30]
O	-1.2	Composition dependent	−0.945
Si	2.4	1.89	1.89
B	1.8	Composition dependent	1.4175
Al	1.8	1.4175	1.4175
Na	0.6	0.4725	0.4725

To better describe the boron-oxygen interaction and reproduce boron anomaly in borosilicate and boron oxide containing multicomponent oxide glasses, Deng and Du developed a set of composition dependent partial charge potential parameters [29]. In development of boron related parameters, the concept of composition-dependent parameter approach by Kieu et al was adopted but modified to improve the transferability and decrease the fitting parameters. Unlike the Kieu et al approach of composition dependent varying charges, the partial charge of boron is fixed to reduce fitting parameters and to ensure the potential to be compatible with a range of other

oxides that have already been developed [29]. Du potential set adopts O-O, Si-O and other interactions consistent with that of Teter potential's original values with additional refinement by Du and Cormack [40]. The A_{ij} parameter for B-O interaction in Eq. (1) is taken to be composition dependent as a function of boron N_4 and derived in following method:

$$A_{B-O} = \begin{cases} A_1 + t_1 \times (R_{max} - (R_{max} - N_4)^2/R_{max}) + t_2 \times K^2 & R \le R_{max} \\ A_2 + t_3 \times R_{max} \times N_4/R_{max} & R \ge R_{max} \end{cases} \quad (2)$$

where A_1, A_2, t_1, and t_2 are empirical parameters and the values are listed in Table 3. The fraction of four-coordinated boron, N_4 is predicated based on DBX model and R_{max} is the value of R where N_4 achieves the maximum value [14] and it is equal to $\frac{K}{16}$+0.5. To obtain a continuous formula, both parts of Eq. (2) are simultaneously solved at $R=R_{max}$. Thus, the value of t_3 can be calculated using the following equation:

$$t_3 = (A_1 + t_2 \times K^2 - A_2/R_{max} + t_1) \quad (3)$$

Table 3 Empirical Parameters in Eq.2 to calculate Aij of B-O pair

Variable	A_1 (eV)	A_2 (eV)	t_1 (eV)	t_2 (eV)
Parameter	11900.00	12525.00	4350.00	85.00

The atomic charge of boron, the ρ_{ij} and C_{ij} in Eq. (1) remain constant with the change of glass compositions. The values of t_1, t_2, and t_3 parameters from Eq. (2) were fitted by the simulations of binary and ternary borate and borosilicate glasses. Initially, boron related parameters were generated by fitting into boron oxides and other sodium borate crystals. These parameters were further refined by applying the MD simulations of wide range of sodium borate and borosilicate glass systems with varying R and K values to reproduce appropriate boron coordination and other structural properties [29]. Additionally, Du potential adopted a short range correction to overcome the shortcoming of the original Buckingham potential to avoid the overriding of power term over exponential term which causes the unphysical fusion of atom in the melt and non-crystalline solid [41] [29]. It is worth mentioning that in the Du potential set, no cation-cation short range interactions are needed. The only interactions between cations are Coulombic. This further reduced the fitting parameters. The potential has been successfully applied to the six-component sodium calcium zirconium boroaluminosilicate glass[29], [42], [43], also named the

international simple glass (ISG) for nuclear waste disposal, and the multicomponent boron oxide containing bioactive glasses [44]–[46], where the transferability has been tested.

2.2 MD simulation details, structural analyses and property calculations

Molecular dynamics simulations were performed using DL_POLY 2.20 software package developed by Smith and Forester at Daresbury Laboratory, UK[47]. To include parallel testing in the analysis, three random configurations were generated for each of the glass compositions where overlapping atoms were made to push away from each other. These initial structures were subjected to a simulated melt-quench process in a cubic box called simulation cell [48].Each of such simulation cells contained around 10,000 atoms with an initial dimension which can replicate the experimental density of the corresponding glass compositions. In this method, the randomly generated initial glass structures were kept to energy minimize at 0K then to relax at 300K and then were melted at 6000K for Du and Kieu potential with a subsequent cooling down to again at 300K. However, for Bauchy potential, the systems were not heated up more than 3000K in order to confirm a stabilized temperature profile. Similar issue was also reported by Fortino et al. [35]. A nominal cooling rate of 5K/ps was maintained throughout the cooling process which is typically used for these types of systems[49]. At each temperature, the system went under a canonical ensemble (constant number, volume, and temperature (NVT)) for 100 picoseconds (ps), and then followed by microcanonical ensemble (constant number, volume, and constant energy (NVE)) for another 100 ps in order to get equilibration. After the system was cooled to 300K, a relaxation step under an isobaric ensemble (constant number, pressure and temperature (NPT)) was applied with zero external pressure so that any change in density would be possible to observe in the simulated glass. At the final temperature (300K), the trajectory was recorded for every 50 configurations of the last 40,000 steps and this final structure was used to do the structure analysis of the glasses obtained after MD simulations. For short range interactions, the cut-off distance was taken to be 8 Å. The real-space part of the electrostatic interplay described as the long-range interactions were calculated using Ewald sum method with a relative precision of $1x10^{-6}$ and a cut-off distance of 10 Å. An integration of the equations of motion was performed using Verlet Leapfrog algorithm with a time step of 1 femtosecond (fs). The interatomic interactions among the atoms were described by Born model of solid combined with partial-charge pairwise potentials. The three recently developed empirical potentials hitherto discussed were used in order to study the comparative aspects of these potentials for the

MD simulation of wide range of borosilicate glass compositions. The structural analysis including the pair distribution functions (PDF), bond angle distribution (BAD), coordination number (CN) and Q_n distribution were obtained from the method adopted by the study of Deng and Du[28]. The cutoff distances for different pairs were determined taking the first minima of the partial correlation functions. For the sake of rationality of the comparative study, identical value of the cut-off distance for each pair was applied for the short- and medium range structure analysis for all the glass compositions.

The mechanical properties such as bulk, shear and elastic moduli were calculated using the finite difference method where the elastic constant C and elastic compliance S ($S= C^{-1}$) matrix were first obtained. The total number of elastic constants was taken to be 21 by symmetry and final glass structure were deformed from six directions (x, y, z, xy, yz, and zx). The elastic constants were calculated using the LAMMPS simulated package [62]. Voigt, Reuss and Hill are commonly used methods for calculating bulk (B) and shear modulus (G). The values of B and G can be then used to calculate the elastic constant. In Voigt method, which takes the assumption of uniform strain in the system, bulk and shear modulus can be calculated from equation (4) and (5). The Reuss method makes assumption of uniform stress and bulk and shear modulus can be calculated using equation (6) and (7) respectively. The final reported elastic moduli based on the Hills approach which averages the results from the Voigt and Reuss methods [61]. For statistical accuracy, data from three parallel tests with different initial configuration for each of the glass compositions was used. Since glass is isotropic in nature, the overall Young's modulus was taken to be the average of all three axis directions whereas in each direction it was calculated as: $E_k^{-1}=S_{kk}$ (k=1,2,3).

$$B_{Voigt} = \frac{1}{9}(C_{11} + C_{22} + C_{33} + 2(C_{12} + C_{13} + C_{23})) \quad (4)$$

$$G_{Voigt} = \frac{1}{15}(C_{11} + C_{22} + C_{33} + 3(C_{44} + C_{55} + C_{66}) - C_{12} - C_{13} - C_{23}) \quad (5)$$

$$B_{Reuss} = (S_{11} + S_{22} + S_{33} + 2(S_{32} + S_{21} + S_{32}))^{-1} \quad (6)$$

$$G_{Reuss} = 15/(4(S_{11} + S_{22} + S_{33} - S_{12} - S_{13} - S_{23}) + 3(S_{44} + S_{55} + S_{66})) \quad (7)$$

2.3 Glass compositions selected for the study

This work began with the application of the three empirical potential sets discussed in the previous section on two model sodium borosilicate glasses: SBN14 (R=0.79, K=3.75)[27] and $3Na_2O$-B_2O_3-$6SiO_2$ (R=3, K=6) as there exist neutron diffraction structure factor both that can be used to validate the simulated glass structures. To investigate the performance of these potentials sets, a series of ternary sodium borosilicate glasses covering wide range of R or the $[Na_2O]/[B_2O_3]$ ratios, were selected. This series (denoted as SBN in this work) consists of eighteen glass compositions [29] holding a systematic change in the R value from 0.1 to 4 and a constant value of $[SiO_2]/[B_2O_3]$ or K value of 2. The glasses are named as SBN-bxxx, where SBN stands for sodium borosilicate glasses, b stands for b series with constant K=2, and xxx is the R value times 100. For example, for a composition named SBN-b130, it means it is sodium borosilicate glass with K=2 and R=1.3. The initial configuration was randomly generated with either experimental densities (SBN-b10 to SBN-b130) or theoretical ones (SBN-b140 to SBN-b400) [29] when the experimental densities are not available. The reason behind choosing this particular series of glasses was to be able to test the potentials over a wide range of R value and to reproduce the variation of boron N_4 as a function of R, while earlier evaluation of potentials only used a few isolated compositions without systematic changes [35], [36]. Alumina is a common oxide in oxide glasses and often co-exist in silicate glass compositions. To further test the potentials, a series of sodium boroaluminosilicate glasses (denoted as SBNA) were also studied by the three potential sets. We adopted the alumina parameter added to the Kieu potential set [27] by Deng and Du [28] but still named it Kieu potential here. This series of glasses has a fixed amount of sodium oxide, while gradually replacing silica by boron oxide, and glass compositions are expressed as $16Na_2O$-$8Al_2O_3$-$4xB_2O_3$-$4(19-x)$ SiO_2 where x=3, 4, 5, 6 all in mol%.

3. Results

3.1 Neutron diffraction structure factors

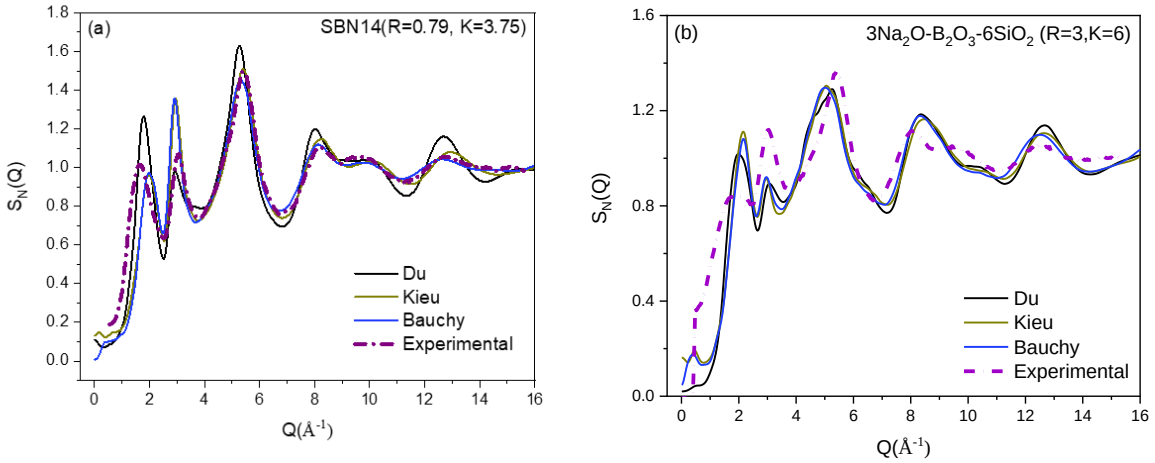

Figure 1 Comparison of structure factors from experiment and three different potential sets for (a) SBN14(R=0.79, K=3.75) and (b) $3Na_2O$-B_2O_3-$6SiO_2$ (R=3, K=6) glass composition

Neutron diffraction structure factors ($S_N(Q)$) obtained from the MD simulations of the two sodium borosilicate glass compositions: SBN14 and $3Na_2O$-B_2O_3-$6SiO_2$, using Du, Kieu, and Bauchy potential sets are compared with the experimental structure factor [27] in Figure 1(a) and Figure 1(b) respectively . These neutron structure factors were calculated using the pair distribution function obtained from the MD simulated glass structures through Fourier transformation method with Lortch type window functions[52]. The first sharp diffraction peak (FSDP) provides information for the medium-range structure information whereas peaks at higher Q shed light on the structural information in short-range. For SBN14, the experimental consists of major peaks around 1.60Å, 3.05Å, 5.45Å and 8.26Å. Three of the potential sets were able to reproduce the peaks at similar positions to that of the experimental curve but there are differences in the peak intensities for all of them. The first peak in the experimental plot (FSDP) is much broader. Du potential was able to produce a broader first peak. Therefore, Du potential could predict more reliable medium-range structure information such as ring size than the other two potential sets.

In another study by Lee et al. [36], where a comparison of Du and Bauchy potential sets was established for a pair of aluminoborosilicate glass system, a better agreement of Du potential at FSDP was reported indicating a more realistic ringsize information. On the other hand, for higher Q value, Bauchy potential was reported to be in better agreement with the experiment data.

3.2 Simulations of sodium borosilicate glasses

The following section discusses the comparison of Du, Kieu, and Bauchy potential sets in MD simulations of the ternary sodium borosilicate system with R from 0.1 to 4 and K=2. Figure 2 shows snapshots of the simulated structure of SBN-b1130 where the structure is made up of networks of [SiO_4], [BO_3] and [BO_4] units linked through corner sharing. Fig. 2(b) shows the zoomed in image of local connections of these structural units. Na ions are located at intestinal sites and play the role of charge compensator to [BO_4] or creates non-bridging oxygen (NBO).

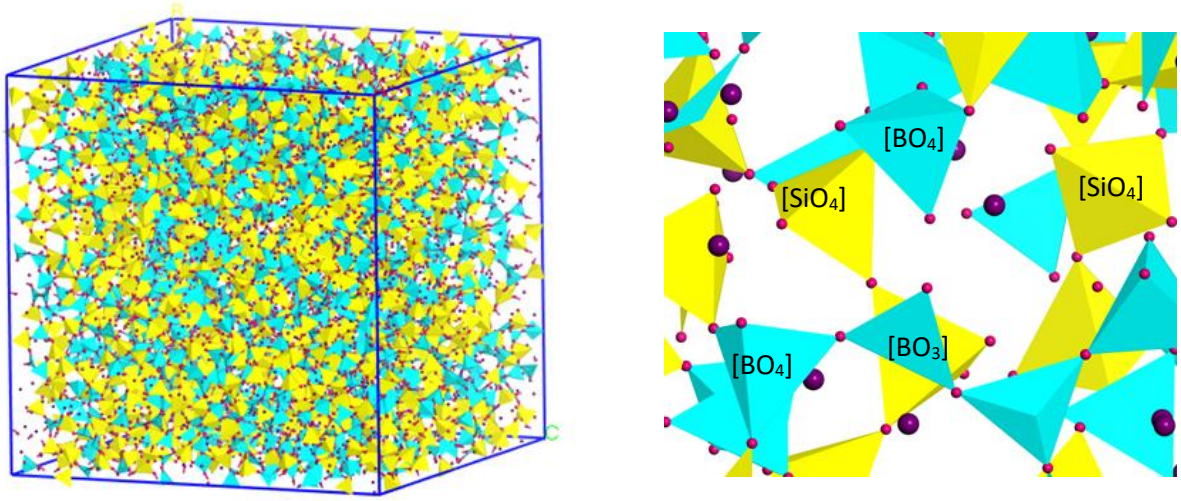

Figure 2 Snapshot of the MD simulated glass structure of SBN-B130 glass using Du's potential (a) full image of the simulation cell with 10,000 atoms (b) a zoomed in snapshot showing [SiO_4] (yellow), [BO_4] (green), oxygen (pink) and sodium (purple)

3.2.1 Change of boron N_4 with glass composition

As discussed earlier, the fraction of four-coordinated boron (N_4) varies with the glass composition following a trend described by Dell, Bray and Xiao (DBX) model. The relationship between $B^{[3]}$ to $B^{[4]}$ conversion and glass compositions can be manifested by the N_4 vs. R (Na_2O/B_2O_3) plot. These plots drawn from the MD simulations of the ternary sodium borosilicate glasses ($0.1 \leq R \leq 4$ and K=2) using Kieu, Du and Bauchy potentials are compared with the DBX model as well as the available experimental values of the corresponding compositions and represented in Figure 3. It can be observed that, up to around R~0.7, all the three potentials are satisfactorily being able to reproduce the trends of DBX model and experimental values. Kieu potential causes an abrupt drop from an overestimated N_4 at around R~1.0 and in the later part of

graph with higher R values, it gives an overall overestimated amount of four-coordinated boron from both DBX model and experiments. Du potential well reproduces the N_4 trend in the whole R ranges with values consistent with the DBX model and experimental values, with only. slight overestimation of N_4 at around the maximum. Following the DBX model, For Du and Kieu potential the N_4 value increases linearly and reaches a maximum and then decreases with increase of R indicating conversion of B_4 to B_3. However, in case of Bauchy potentials, despite good agreement with the DBX model for small R values before the plateau, the N_4 from this potential does not show a clear plateau and then decrease trend but instead continue to increase monotonically with R. This might be due to the fixed parameter that was not able to reproduce the B N_4 trend with R in wide composition ranges hence to describe properly the boron anomaly. The results thus indicate that the Du potential provides most favorable agreement of boron coordination change with composition that shows the best agreement with the DBY model and NMR values. Kieu potential shows general agreement of trend but there are variations with the model in the high R value range around and after the plateau. While Bauchy potential only works for small R values before the plateau. At and after the plateau, it provides wrong trend of B N_4.

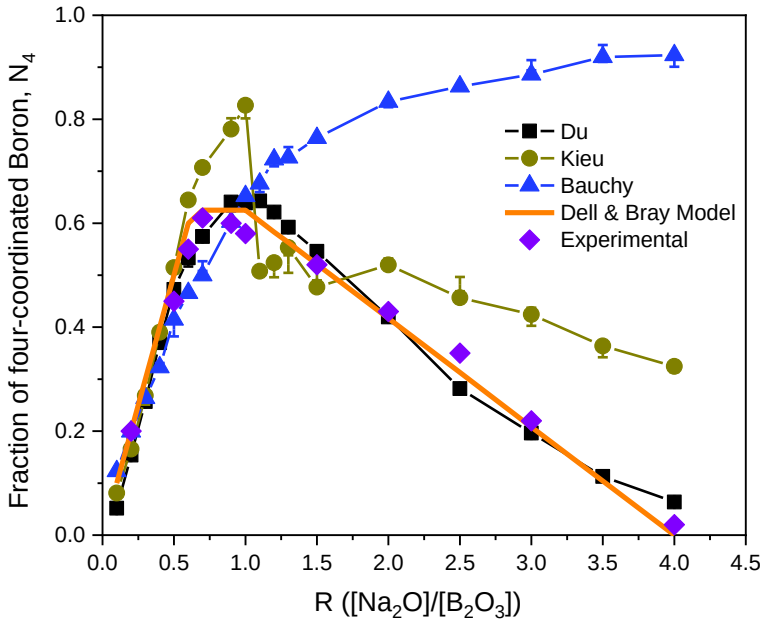

Figure 3 Fraction of four-coordinated boron, N_4 as a function of R (Na_2O/B_2O_3) at K(SiO_2/B_2O_3) =2 obtained from three different potentials (Du, Kieu and Bauchy), DBX model and experiments in Na_2O-B_2O_3-SiO_2 ternary glass system

3.2.2 Partial Correlation Functions

In addition to the boron coordination, the local environment of B and other cations can be studied by calculating the pair distribution functions. Figure 4 shows the partial correlation function T(r) of all the cation-oxygen and oxygen-oxygen pairs in the simulated structure of SBN-b130 glass composition (R=1.3). The first major peak indicates the bond distance of the corresponding pair. The values of these bond distances are listed in Table 4. All the three potential sets were able to bring about Si-O distance of ~1.61 Å which is consistent with experimental findings[53]–[55].

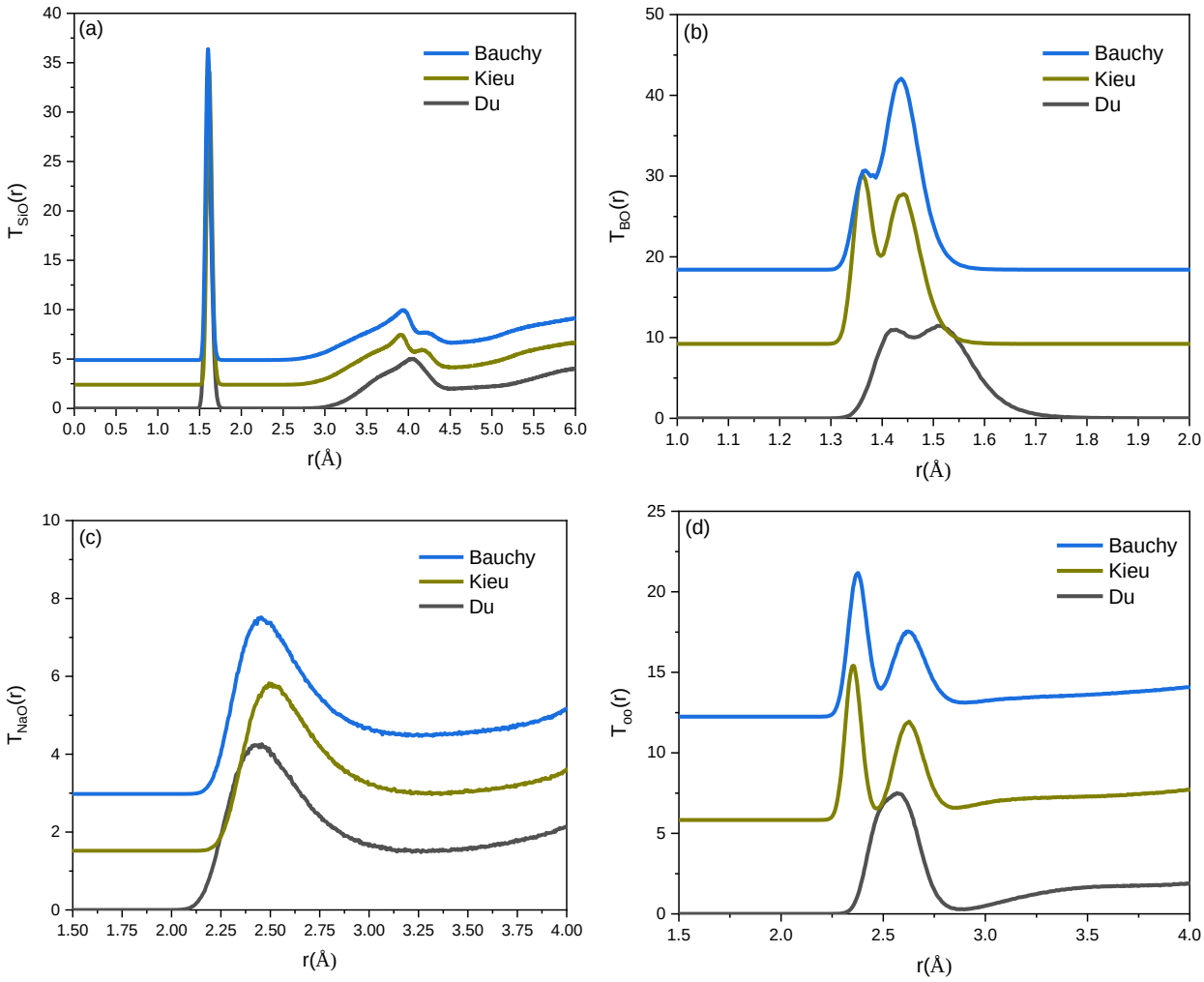

Figure 4 Total correlation functions of (a) Si-O, (b) B-O (c) Na-O and (d)O-O pairs in simulated SBN-b130 glass composition (R=1.3)

Table 4 Bond Lengths of the pairs in simulated SBN-b40 (R=0.4, K=2)/SBN-b130 (R=1.3, K=2) glass composition and corresponding values obtained from the references

Bond Length, Å	Du	Kieu	Bauchy	Exp.	*ab initio*
Si-O	1.608/1.608	1.603/1.618	1.628/1.603	1.60-1.61[54]	1.64[35]
$B^{[3]}$-O	1.443/1.423	1.383/1.363	1.453/1.368	1.37-1.38[56], [57]	1.37[58]
$B^{[4]}$-O	1.538/1.518	1.393/1.443	1.463/1.438	1.48-1.49[56], [57]	1.47[58]

The partial correlation function of B-O pair has a bimodal distribution for all of the three potentials. The peak at shorter distance and the one at longer distance represent tri- and tetra-coordinated boron respectively. Figure 5 shows a typical deconvoluted $B^{[3]}$-O and $B^{[4]}$-O peaks in the partial correlation function of B-O obtained using Kieu potential. Du potential set shows slight composition (and N_4) dependent B-O bond distance and it overestimates both the $B^{[3]}$-O and $B^{[4]}$-O bond distances by around 0.05 Å as compared to the experimental and *ab-initio* simulations for some compositions, while the difference between $B^{[3]}$-O and $B^{[4]}$-O bond distances is around 0.1 Å, in good agreement with experiment or *ab initio* data. Kieu potential was able to reproduce $B^{[3]}$-O and $B^{[4]}$-O bond distances with a deviation within ~0.01 Å and ~0.04 Å respectively with the experimental and *ab-initio* references. Bauchy potential reproduced the $B^{[3]}$-O distance in good agreement with experiments but the $B^{[4]}$-O distance is 0.04 Å shorter, which led to the bond distance between the two boron coordination states of 0.07 Å, shorter than 1.0 Å from experiments. Due to the usage of fixed parameter, the bond distance of models from Bauchy potential do not show composition dependence. The peaks of $B^{[3]}$-O and $B^{[4]}$-O from all three potentials are also in good agreement with the amount of N_4 yield for this particular composition (R=1.3, K=2). Comparing Figure 3 and 4, Du potential brought about around ~60% of boron N_4 having close intensities of these two peaks of B-O bond distances. For Kieu potential, ~55% of N_4 resulted in a higher peak intensity of $B^{[4]}$-O bond distance. In case of Bauchy potential, around ~73% of N_4 was produced giving rise to an intense peak of $B^{[4]}$-O bond distance.

One interesting feature can be observed from O-O partial correlation functions of these potentials. O-O partial distribution is formed by the contributions of $B^{[4]}$-O, $B^{[4]}$-O and Si-O bond distances [58]. In cases of Kieu and Bauchy potentials, the first peak of O-O distribution

shows bimodal distribution. Here, the shorter distance peak at 2.36 Å and longer distance peak at 2.61 Å correspond to contributions of O-O interactions in BO_3/BO_4 and SiO_4, respectively. Due to the fact that Du potential set overestimates the B-O bond distance at this particular glass composition, the O-O interactions of the two types of polyhedra merged into a single peak [36].

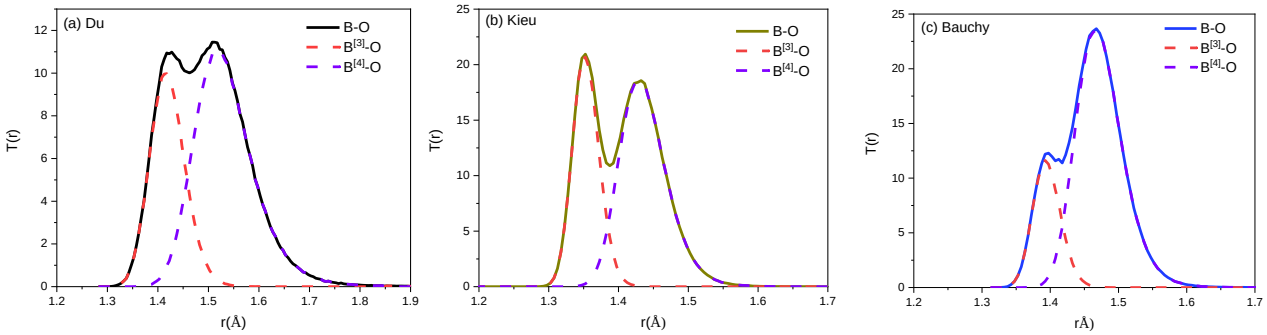

Figure 5 Deconvoluted B-O partial correlation function for SBN-b130 (R=1.3) glass composition using Du, Kieu, and Bauchy potential sets. The three and four-coordinated boron are distinguished by red and purple dashed lines respectively

3.2.3 Bond angle distribution

Bond angle distributions of the polyhedral provide further details of the local coordination environment of cations and how they are connected together. Figure 6(a) shows the O-Si-O bond angle distribution of one of the simulated compositions SBN-b130 (R=1.3, K=2) using three different potential sets. It has a defined peak located around ~109.5° for all three potentials which is close to the theoretical value of perfect tetrahedron. This is consistent with the closes to perfect four-fold coordination of Si in all the potentials. Figure 6(b) shows the bond angle distribution of O-B-O for the same glass composition. For all three potential sets, this bond angle distribution shows two major peaks. The first major peak is located around ~109.5° corresponding the four coordinated boron [BO_4] which forms perfect tetrahedrons. The next major peak corresponds to three coordinated boron which is located around 120° indicating [BO_3] triangles. The positions of both of the peaks are same for all of the three studies potentials but intensities of a particular peak are different for different potential set. This is as a result of their varying percentages of boron species.

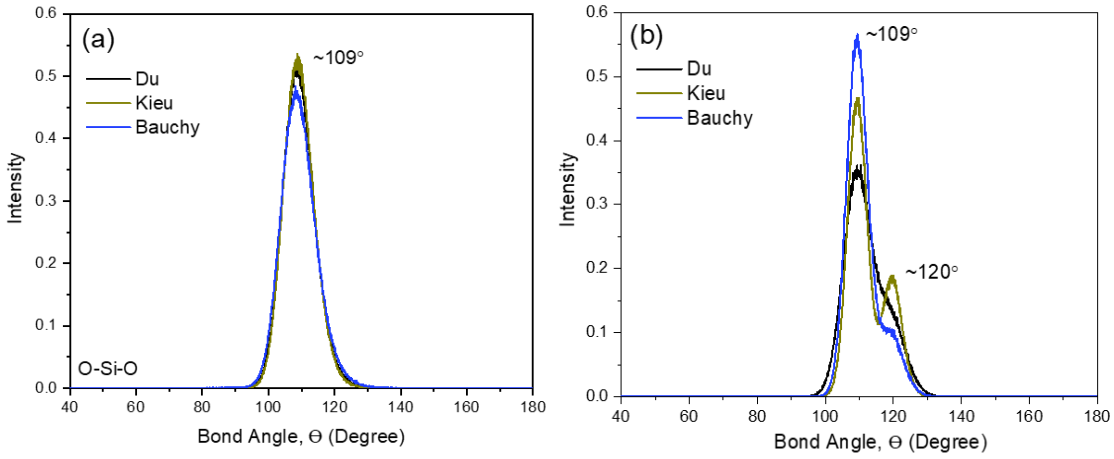

Figure 6 (a) O-Si-O and (b) O-B-O bond angle distribution for SBN-b130 (R=1.3) glass composition using three different potentials

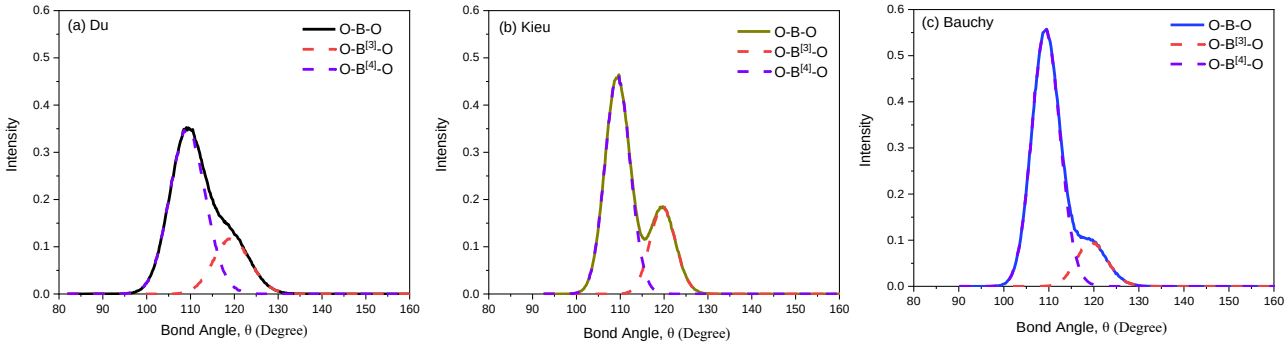

Figure 7 Decomposed plot of O-B-O bond angle distribution for SBN-130 (R=1.3) glass composition using Du, Kieu, and Bauchy potential. Three- and four-coordinated boron are distinguished by red and purple dashed lines respectively

Figure 7 is a deconvoluted plots of O-B-O bond angle distribution for this compositions using three of the potentials decomposed into O-$^{[3]}$B-O and O-$^{[4]}$B-O bond angle distributions located at 120° and 109.5° respectively. These peak positions obtained from all three potentials are in well accordance with the simulation results of sodium borosilicate [26], *ab initio* findings [30] and experimental values [56].

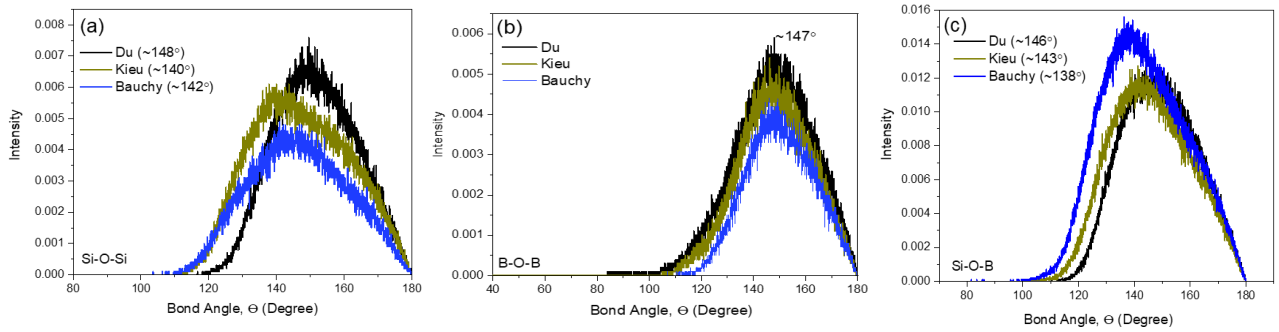

Figure 8 Si-O-Si, (b) B-O-B, and (c) Si-O-B bond angle distributions for SBN-130 (R=1.3) glass composition using three different potentials

Figure 8 illustrate the bond angle distributions of Si/B-O-Si/B of the SBN-b130 (R=1.3) glass composition using three different potentials. These bond angle distributions range from 90° to around 180° all having a single peak. Three different potentials result in difference in the intensities of the peaks whereas the peak positions remained to be similar. Comparing intensities of the peaks from Figure 8 (a), (b) and (c), Si-O-Si bond angle distributions show a higher intensity than that of Si-O-B or B-O-B which indicates that Si-O-Si linkages is the most preferred one which is also in accordance with previous simulation results [28].

3.2.4 Change in densities with R and K

Since the MD simulation method consisted of a relaxation step by NPT ensemble, it is possible to capture density information from the end structure of the glass and hence can be compared with the experimental data. Figure 9 shows the final densities of the simulated glasses obtained using three sets of potentials as a function of R ($[Na_2O]/[B_2O_3]$) for K($[SiO_2]/[B_2O_3]$) =2 compared to the experimental (SBN-b10 to SBN-b130) and theoretical (SBN-b150 to SBN-b400) densities of the corresponding compositions. All the three potentials were able to result in final densities which give rise to the general trend exhibited by experimental values as a function of R. Du potentials reproduced the densities closest to the experimental values with a difference lying within ~0.05 g/cm^3.Kieu and Bauchy potentials result in final densities of the simulated glasses which are higher than experimental ones and the dispersions are within 0.22 g/cm^3 and 0.18 g/cm^3respectively. For all of these three potentials, the deviation from the experimental data seems to be diminished with the increasing value of R.

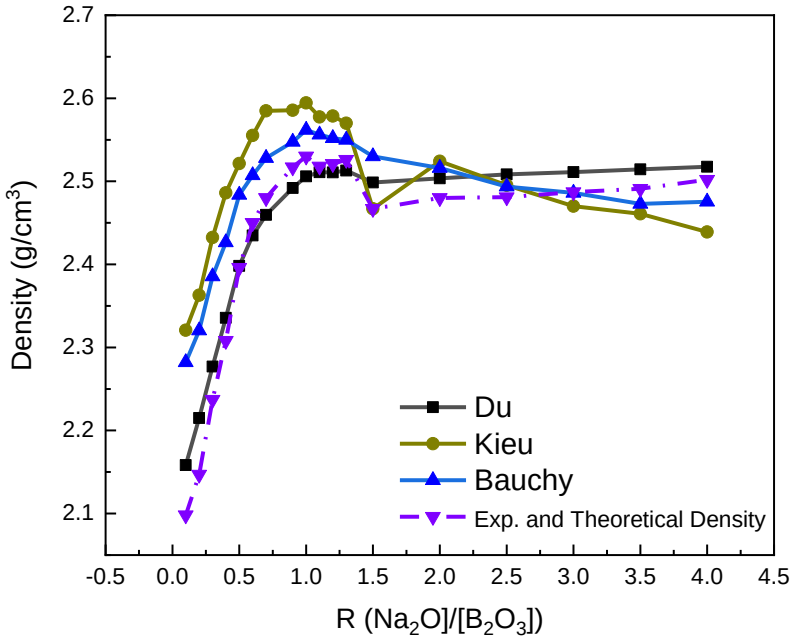

Figure 9 Densities of the simulated glasses a function of R ([Na_2O]/[B_2O_3]) at K([SiO_2]/[B_2O_3])=2 obtained from three different potentials(Du, Kieu and Bauchy) and experiments in Na_2O-B_2O_3-SiO_2ternary glass system

3.2.5 Fraction of non-bridging oxygen

The environment around the glass former (boron and silicon) was further investigated by calculating the fraction of non-bridging oxygen in the surrounding at different R values with constant K=2. These fractions were obtained by taking the ratio between the non-bridging oxygen to the total oxygen. The results obtained from the glasses simulated by using Du, Kieu and Bauchy potential set were compared with the ones calculated from DBX model and shown in Figure 10. As discussed earlier, sodium first converts three-coordinated boron to four-coordinate, then keeping the four-coordinated boron fixed, it produced non-bridging oxygen for the silicon and finally four-coordinated boron is converted to three-coordinated boron while increasing the non-bridging oxygen for both boron and silicon. All of the potential sets were able to reproduce this trend where with higher sodium content i.e. increasing R, the fraction of non-bridging oxygen increased. But the amounts of non-bridging oxygen at a particular R value are different for three different potential sets. Du potential set is in the best agreement with the DBX model. Kieu potential set agrees DBX model better at low sodium content but later on shows a

maximum discrepancy of ~5%. For Bauchy potential, a maximum mismatch of ~18% is observed.

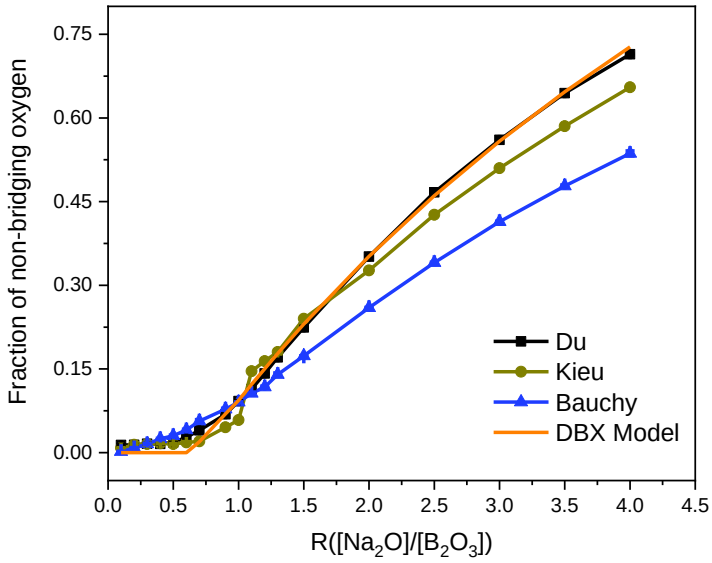

Figure 10 Fraction of non-bridging oxygen around glass former atoms as a function of R at K=2 from three different potentials sets and DBX model

3.2.6 Local environment around Sodium

The role of sodium in this ternary system can be explained by DBX model [14]. At first the sodium will start converting the three-coordinated boron into four-coordinated boron resulting in a positive slope of N_4 vs. R curve. Then, after reaching a maximum of N_4, the excess of the sodium starts to produce non-bridging oxygens for silicon, unaltering the N_4 which is indicated by the plateau region in DBX curve.

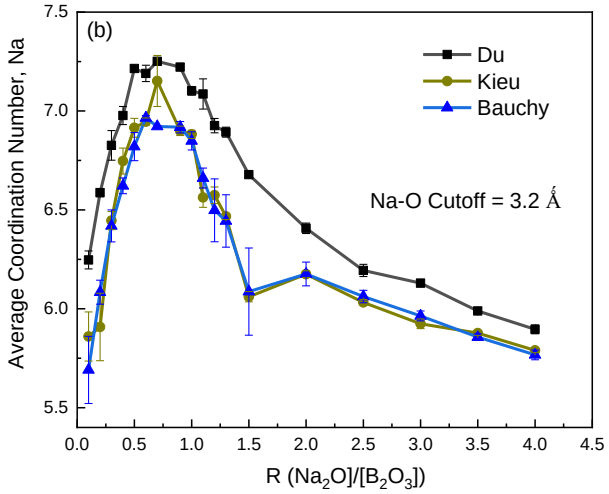

Figure 11 Average oxygen coordination number around sodium as a function of R obtained for Du, Kieu and Bauchy potential. The error bars are calculated from the standard deviation of the three parallel tests

Finally, with addition of more sodium, the four-coordinated boron will revert back to three-coordinated boron while the excess of sodium will generate non-bridging oxygen for both silicon and boron. As described by Stebbins [59], the higher the non-bridging oxygen to glass formers ratio, it is likely there will be more oxygen in the first coordination shell of the sodium. Due to the strong covalent nature of the bond between non-bridging oxygen with sodium, Na-O distance decreases with increasing non-bridging to glass former ratio as observed in the third stage of DBX curve. Therefore, depending on the role of the sodium in the glass (either as a charge compensator or glass modifier) the Na-O distance varies.

3.2.7 Ring Size Distribution

Primitive ring size distribution is a medium range structure information of network forming glass structures[41], [60]. For example, pure silica shows a systematic distribution of 6-membered ring and with addition of modifier oxides to the network, the intensity of the major peak decreases and larger membered rings are formed. The primitive ring size distributions of the simulated glass structures using three different potentials were analyzed for SBN ternary systems. For SBN-b40 (R=0.4, K=2) and SBN-b110 (R=1.10, K=2) glass compositions the ring size distribution obtained from these potentials are illustrated in Figure 12. The analysis was performed considering the linkages between Si-O and B-O with their corresponding cut-off

values from the pair distributions functions. In Figure 12 (a), ring size is distributed from 2 to 16 membered rings the peak lying around ~7 membered rings for all three potentials sets though Du and Bauchy potentials show irregularities around the the peak position. With the addition of more Na_2O i.e. with increasing R, the ring size distributions broadens in Figure 12 (b). Even though in this case, the peak position of the ring size distributions still remains around 7-remembered rings, there is an increase in the larger membered rings extending the ring size distribution up to 18 to 19 membered rings.

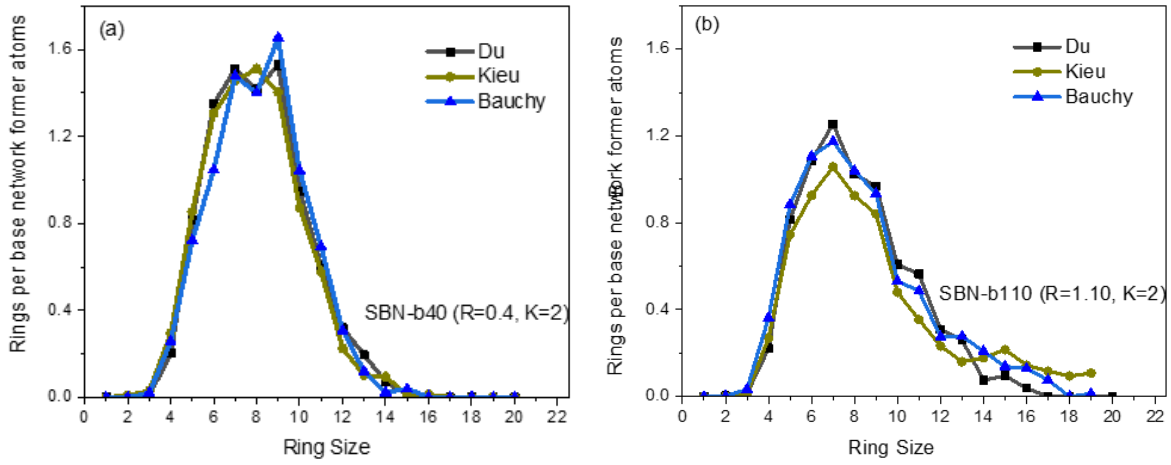

Figure 12 Ring size distribution of (a) SBN-b40 (R=0.4, K=2) and (b) SBN-b110 (R=1.10, K=2) glass compositions using three different potentials

3.2.8 Mechanical Properties

The calculated values of Young's, bulk and shear moduli as a function of R of the simulated glasses using three different sets of potentials can be shown in Figure 13. Also, the available experimental data [63] for these moduli (for compositions with R up to 1.3) has been plotted along for comparison. Following similar trend of the B N_4, these moduli increase with R and reach maximum and then decreases with increasing sodium content in the glass compositions. The maximum occurs around the R=0.625, which is also equal to the R_{max} (equals to $\frac{K}{16}$ +0.5) or highest point of the DBX model referring to the largest fraction of four-coordinated boron (N_4).

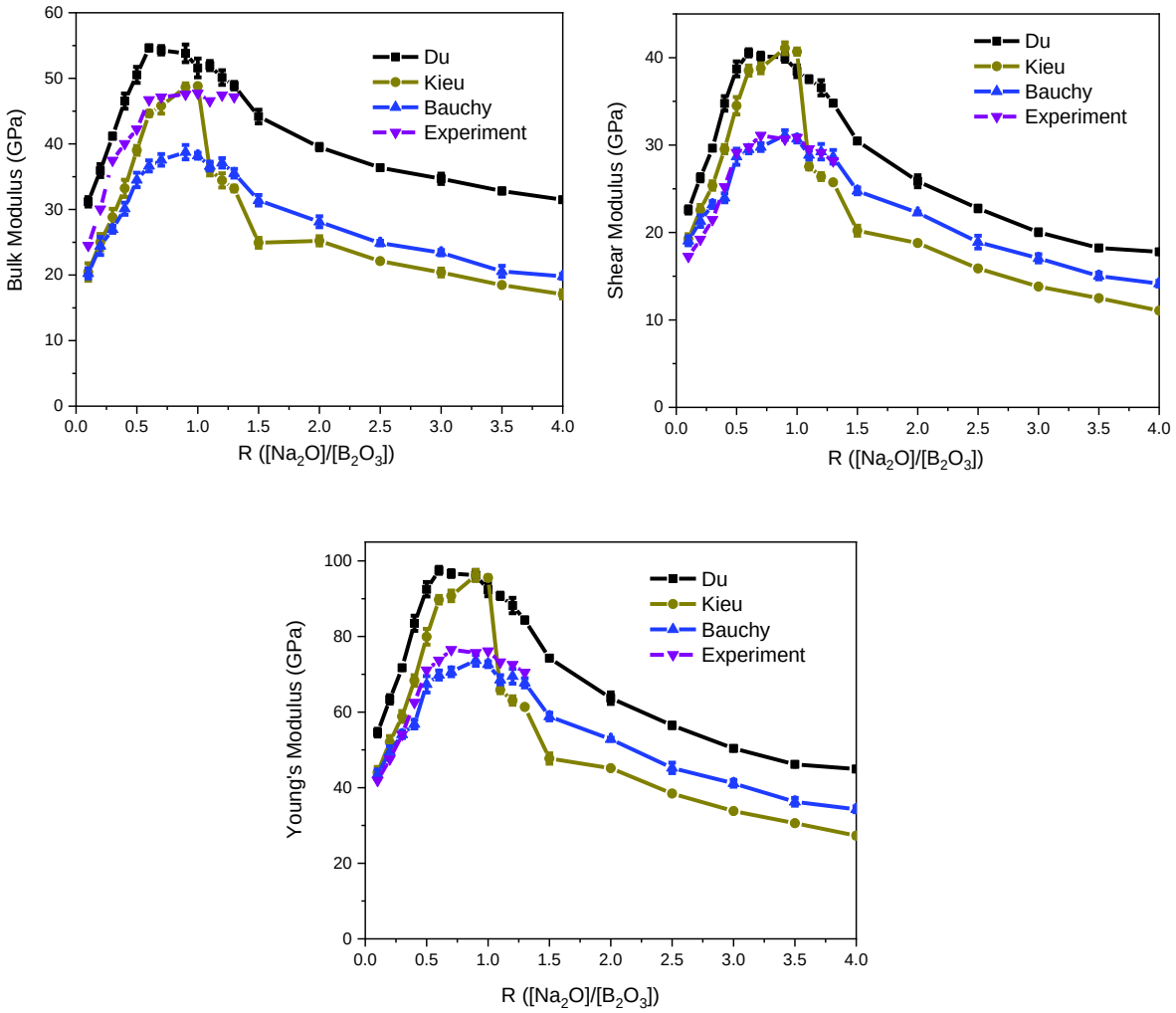

Figure 14 Comparison of the mechanical properties (a) Young's modulus, (b) bulk modulus and (c) shear modulus of the simulated glass from three potentials and experimental data (for R from 0 to 1.3) [63]. The error bars are calculated from the standard deviation of the three parallel tests

The general trend of the experimental moduli with compositions are well reproduced by Du, Kieu and Bauchy potential sets. Du's potential provides reasonable prediction of elastic moduli at small R (R<Rmax) but in general overestimates the values of the moduli in plateau region around R_{max} (equals to $\frac{K}{16}$ +0.5) and those with larger R values. Similar overestimation of the moduli was observed by Kieu's potential around the plateau region but after R_{max} the predicted moduli becomes smaller than experiments, showing an abrupt decrease that is related the treatment of the potential when approximating the DBX model (this can be seen in Fig. 3). Bauchy potential significantly underestimates bulk moduli but has good agreements with experiments for shear and Young's moduli (for the range with experimental data). All three potentials show the decrease trend of moduli at larger R after the plateau. This is understandable

for Du and Kieu potential as the boron coordination shows similar trend (Fig. 3). Bauchy potential predicts continuous increase of B N_4 with R, opposite to the DBX model, at larger R, the calculated elastic moduli somehow defy the trend of N_4 and comes down with R. Overall, all the potential sets give good prediction of the moduli as a function of R up to R_{max} but differ in behaviors for compositions with higher soda content and larger R values. Improvements are needed in future refinement of the potentials parameters to better reproduce the mechanical properties.

3.3 Simulations of sodium aluminoborosilicate glasses

To further evaluate the three sets of potential, they were used to simulate a series of sodium boroaluminosilicate glasses which can be expressed as the formula $16Na_2O$-$12Al_2O_3$-$4xB_2O_3$-$4(19-x)$ SiO_2 where x=3,4,5,6 in similar simulation method applied for the ternary system [28]. Some of the results and findings are discussed in the following sections.

3.3.1 Partial Correlation Functions

Figure 14 illustrates the partial correlation functions of oxygen related pairs in the simulated SBNA3-5 glass composition from boroaluminosilicate series. The peak position indicates the bond distance of oxygen and the corresponding cation. All three potentials sets result in a Si-O bond distance around ~1.61Å with a good accordance with other simulations of boroaluminosilicate glasses [41], [64]. Al-O partial correlation function peaks around 1.76Å, 1.73Å, and 1.74Å for Du, Kieu, and Bauchy potentials, respectively. These values are in good agreement with the experimental finding collected by EXAFS analysis of sodium boroaluminosilicate glasses [65] . For Al-Al pair, there is an appearance of a shoulder at ~2.5 Å for Bauchy's potential. It could be due to presence of two-membered ring or edge sharing of aluminum oxygen polyhedra. It is worth pointing out that noticeable differences of first peak of O-O partial correlation functions from the three potentials: Du potential shows a single peak with a shoulder on the smaller r side while Kieu and Bauchy potential show two distinct peaks. This might be related to the B-O bond distances of the three potentials discussed earlier in the ternary systems.

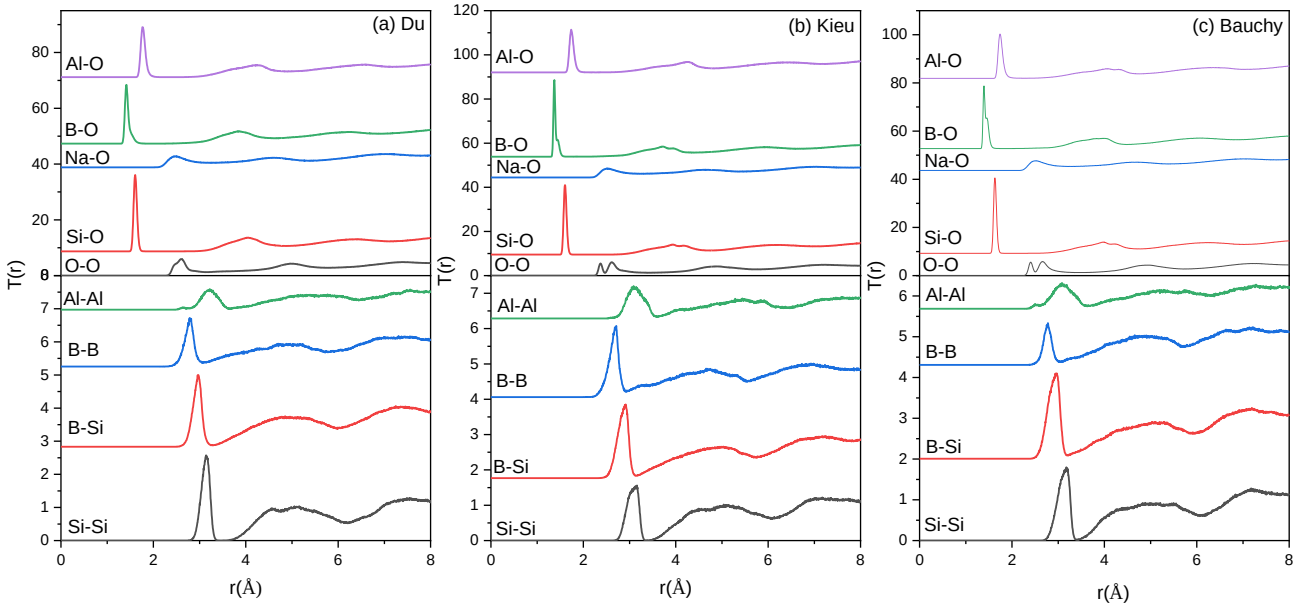

Figure 15 14 Partial correlation functions of oxygen related pairs for SBNA3-5 glass composition using (a) Du, (b) Kieu, and (c) Bauchy's potential

3.3.2 Coordination environment of the glass formers

As discussed earlier, due to the presence of aluminum in these glasses, sodium should first charge compensate $[AlO_4]^-$ tetrahedral units. Table 5 reports the obtained percentages of three- and four coordinated boron and average oxygen coordination number of aluminum in the simulated glasses using three different sets of potentials. With increasing percentage of B_2O_3 number of three coordinated boron ($^{[3]}B$) increased since more and more boron were left to be not charge compensated. But the percentage of two of the boron species vary for different set of empirical potentials. All three of these set were able to reproduce the aluminum coordination with oxygen in the correct manner which remained to be four.

Table 5 Boron speciation and average Aluminum coordination in SBNA series from MD simulations and those from the Du and Stebbins model

Glass	SBNA3-3			SBNA3-4			SBNA3-5			SBNA3-6		
Potential sets	Du	Kieu	Bauchy	Du	Kieu	Bauchy	Du	Kieu	Bauchy	Du	Kieu	Bauchy
% of $B^{[4]}$ Species	25.8	35.1	51.4	26.3	25.7	44.2	18.5	23.1	40.2	13.6	18.5	37.6
Average Al coordination.	4.003	4.003	4.091	3.999	4.007	4.101	4.011	4.002	4.086	4.005	4.005	4.138
Simulated N'_4 values	62.4	66.9	71.5	53.9	57.0	64.4	44.3	51.3	59.4	37.9	45.2	54.6
N'_4 values from model	65.6			57.1			50.0			44.4		

As discussed earlier, Du and Stebbins [19] model can be applied to boroaluminosilicate glass systems with modified R and K values. Since the four-coordinated aluminum exhibits similar network forming property as four-coordinated boron, this model treats both of these species as one general type. Therefore, the modified R and K values denoted as R' and K' respectively can be defined as following [28],

$R' = Na_2O/[B_2O_3+Al_3O_3]$ (7)

And, $K' = SiO_2/[B_2O_3+Al_3O_3]$ (8)

Also, the modified N'_4 which is the fraction of four-coordinated boron and four-coordinated aluminum, can be expressed as:

$N'_4= N_4*[B_2O_3+Al_3O_3] /[B_2O_3+Al_3O_3]$ (9)

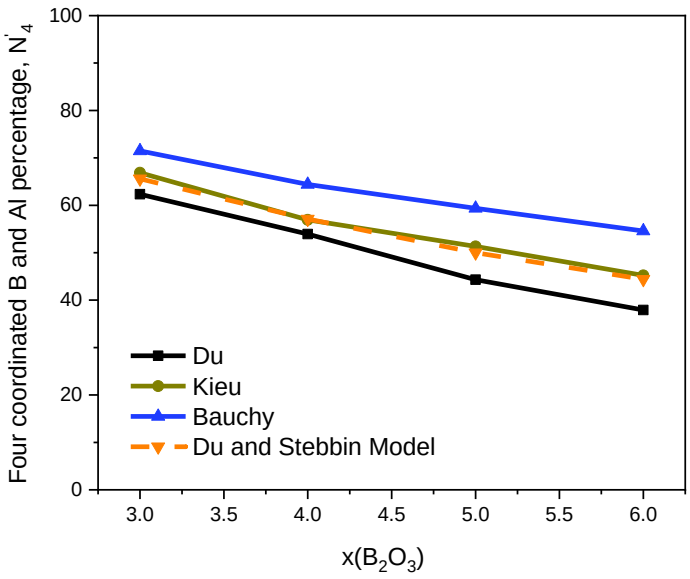

Figure 16 Theoretical N'_4 (percentage of four coordinated B+Al calculated from Du and Stebbins model) and simulated N'_4 values as a function of x = 3,4,5,6 (B_2O_3 concentration)

Figure 15 shows a comparison of and N'$_4$ calculated for simulated SBNA3-5 glass composition using three different potentials as well as N'$_4$ calculated from Du and Stebbins model using equation (9). It can be seen that, Kieu potential set (with the addition of Al parameters by Deng and Du) has the best agreement with the Du and Stebbins model. Du potential set shows a discrepancy around ~6.5%. For Bauchy potential set shows mismatch around ~10%.

3.3.3 Mechanical Properties

Mechanical properties of the simulated SBNA glass series using the three different potentials were calculated using the method introduced earlier. The calculated mechanical properties in terms of Young's, shear, and bulk modulus together with available experimental data [66] are plotted in Fig. 16. Except the composition with 16 mol% B_2O_3 which is clearly an outlier in experimental data, in general, all three potential sets show similar trend of Young's, shear and bulk moduli as a function of composition and are in good agreement with experiments, indicating their ability to predict mechanical properties of the quaternary systems. There are differences of subtle details: Du potential overestimates the elastic moduli by 5-10 GPa while Kieu potential slightly underestimate the moduli and Bauchy potential is in between. Together

with earlier observations [28], this shows directions of future improvement of the potentials to give better predictions of the mechanical properties.

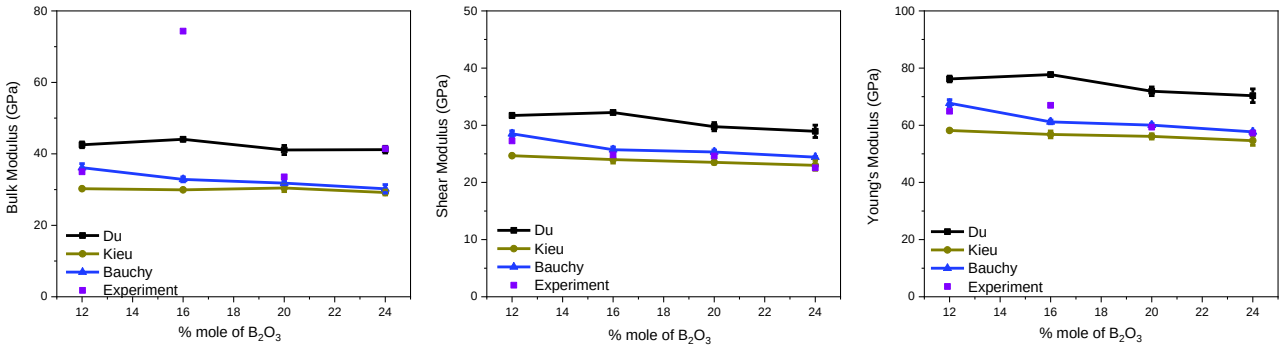

Figure 17 Comparison of the mechanical properties (a) Young's modulus, (b) shear modulus and (c) bulk modulus of the simulated glass using Du, Kieu, and Bauchy's potentials. The error bars are calculated from the standard deviation of the three parallel tests

4. Discussion

Being a highly valuable tool to investigate the structures and properties of glasses and amorphous materials, successful applications of molecular dynamics simulations rely on the availability and quality of empirical potentials. This work focuses on comparison of three available (including two recently developed) potentials on their ability to simulate sodium borosilicate and boroaluminosilicate glasses. We also need to keep in mind that the structure and properties of glassy materials are thermal history dependent. It is well known that, the cooling rate in MD simulations during glass formation is usually orders of magnitude higher than experimental values of normal melt and quench processes. Therefore, a debate remains about the reliability of the simulated glass structures. Important features of borate glasses such as N_4 as well as their mechanical properties are indeed found to be system size and cooling rate dependent [49]. With all glasses generated with similar system size of around 10,000 atoms and the same cooling rate of 5K/ps, this comparative work mainly focused on the trend and change in the trend with composition of glasses more than matching the exact values with the experiments.

Constant pressure or constant volume ensembles are commonly used in MD simulations to generate glass structures with the simulated melt and quench approaches. Since constant pressure simulation creates a much stricter simulation environment, some potential sets become unstable

in this process, especially at high temperatures. This work adopted constant volume ensemble during cooling with a constant pressure relaxation at room temperature for all the potential sets. The Bauchy potential needed to adopt a lower melting temperature of 3000K due to system instability at higher temperatures. In general, all three potential sets have been used to simulated a diverse range of sodium borosilicate and aluminoborosilicate glass systems in this work. In general, all three potential sets were able to generate overall reasonable glass structures but there are also subtle yet significant differences.

This systematic study provides a quantitative evaluation of the three potential sets for borosilicate and boroaluminosilicate glass systems. The potentials were tested in a ternary sodium borosilicate glass system (SBN series) with R varying from 0.1 to 4 and constant K (=2) value to observe their ability to reproduce the trend of three- and four-coordinated boron conversion with glass compositions as seen in DBX model and experiment. From Figure 3 we observe that, all of the potential sets are capable of reproducing the trend of DBX and experimental data therefore N_4 increases with increasing R up to R~0.7. Du potential provides the best agreement in terms of boron coordination in the whole composition range: showing initial linear increase of N_4 with R, a plateau and then decrease in N_4. With higher R and close to the plateau region, Kieu potential showed similar shape but relatively large differences as compared to the DBX model and experimental values of N_4. This is likely due to the conversion of the DBX model to analytical expressions that introduced errors in Kieu potential. Bauchy potential set, although also capable to describe the N4 increase with R in low R values, on the other hand, shows a monotonic increase of N_4 with R, different from the DBX model and experimental values. The reason behind this behavior can be due to the nature of this potential: that is, it uses fixed parameter for boron to achieve greater transferability. While simple and easy to use, Bauchy potential loses the accuracy of describing boron coordination change in compositions with large R values hence its transferability. The reason why some of the simulated glass provide reasonable boron coordination could be due to the fact that these studies happened to be on glass compositions where the potential works pretty well. Therefore, while making a choice of potential set for MD simulation, one should keep in mind that performance of this potential set is dependent on the glass composition, especially in wide composition ranges.

For sodium aluminoborolisicate systems, the boron N_4 from glasses generated with different potential sets were compared with those from the Du and Stebbins model and reported in Figure 15. For quaternary systems containing alumina, the fraction of four-coordinated boron and four-coordinated aluminum (N'_4) was considered. Kieu potential set shows best agreement of this model whereas Du potential shows a mismatch of around 8%. Bauchy potential set shows highest mismatch with the model. Except for its constant boron parameters, another reason may play a role in the mismatch in reproducing boron coordination. As mentioned in the section 2.2, this potential cannot withstand a melting temperature higher than ~3000K in alternating NVT and NVE ensembles. Since structure and properties of glasses are dependent on its thermal history, it would be better to be able to melt them at sufficiently higher temperature to obtain a reasonable structure.

In addition to boron coordination, other structural information of the simulated glasses derived from the potentials sets shed light on their performances. Short-range structure information for example partial correlation functions, bond angle distribution was obtained for the studied glass. As reported in Table 1, Kieu and Bauchy potential results in closer $B^{[3]}$ -O distance with the experimental value, while slightly underestimate the average bond difference between $B^{[3]}$-O and $B^{[4]}$-O. For some glass compositions, Du potential overestimates the average B-O bond length but provides the correct difference between the $B^{[3]}$-O and $B^{[4]}$-O. This also shows indications in peaks of O-O distribution functions behaviors. To further elucidate these differences, high quality experimental data such as neutron diffraction that can reach high Q values in reciprocal space so high resolution first peaks can be obtained in real space to separate the contributions from $B^{[3]}$-O, $B^{[4]}$-O and Si-O would be highly desirable. Due to the abnormal neutron scattering of ^{10}B, ^{11}B enriched samples will be needed for this purpose.

Overall, the tested three potentials can all be used to generate structural models of sodium borosilicate and boroaluminosilicate glasses. They differ, however, in details both in terms of the empirical potential parameterization and capability to reproduce structural details of the two glass systems such boron N_4 value, other cation coordination numbers, bond distance, density and mechanical properties. In general, the Kieu and Du potential adopted the idea of composition dependence of parameters to reproduce the boron coordination change in wide composition ranges and do indeed perform better in those aspects. Bauchy potential has fixed parameters and

does not need composition dependent parameter, thus it is simpler and potentially more transferable, but it was not able reproduce the coordination change of B at certain composition ranges. Particularly, the boron N_4 value should decrease after the plateau compositions from DBX model and NMR studies but Bauchy potential keep on increasing with R, see Fig. 3, which means the potential was not able reproduce the $B^{[4]}$ to $B^{[3]}$ conversion after the plateau. Additionally, Kieu potential shows an abrupt drop of N4 near the end of the plateau (Fig. 3). This abrupt change is due to the quick decrease of the $A_{B\text{-}O}$ (the A parameter of B-O Buckingham interaction). The $A_{B\text{-}O}$ is a function of R* which is a step function. R* becomes discontinuous at R=K/4+0.5 (the end of the plateau in DBX model). As $A_{B\text{-}O}$ is a polynomial function of R*, when R* is discontinuous, $A_{B\text{-}O}$ also shows a sharp drop after the plateau (R=K/4+0.5) [27]. This leads to the abrupt change of B N_4 at the composition with R=K/4+0.5. Fig. S1(a) shows the R* change with R and a discontinuity is obvious at R=1. The $A_{B\text{-}O}$ change with R* is also shown in Fig. S1(b). It shows that at high R* values, $A_{B\text{-}O}$ even becomes negative, hence is not physical as it is the parameter for the exponential repulsion. This was observed before in our earlier study [28].

In terms of potential complexity, Kieu potential is the most complex as it has composition dependent atomic charges and boron short range parameter ($A_{B\text{-}O}$). This followed by Du potential that has fixed charges but a composition dependent parameter for B-O short range interactions, similar to the Kieu potential. However, Du potential does not require cation-cation short range interactions hence has less fitting parameters while such interactions are needed in the Kieu and Bauchy potentials. And it does not have the issues of abrupt B N_4 change as discussed above. Another advantage of the Du potential is that the B-O parameter is compatible with parameter sets for a wide range of oxides (known as the Teter potential) thus can be used to simulate multicomponent borate containing glasses [29]. Bauchy potential for boron is also compatible with a set of other oxides (Guillot and Sator [33]) hence can potentially be used to model multicomponent glasses while Kieu potential is more difficult to add other oxides due to the complex potential form and larger number of fitting parameters. As this manuscript was being prepared, two new potentials were published (one polarizable potential [32] and one fixed charge potential [67]). Future study to include comparison of these new potentials would be valuable for potential development and applications of MD simulations of other borate containing glasses.

5. Conclusions

A comprehensive investigation of the compatibility of three recently developed empirical potential sets for the simulations of borosilicate and boroaluminosilicate glasses in wide composition ranges was performed. These recent developments enabled the MD simulations of boron oxide containing glasses that find wide scientific and industrial interests but their performances differ quite significantly. Although all of them can be used to model the tested glass systems using the simulated melt and quench procedure of glass formation, they differ in the capability to reproduce the change of the fraction of four-fold coordinated boron (N_4 value), fraction of NBO, with composition and the trend of mechanical properties. These potential sets are different in their ways of development and characteristics; therefore, they show differences in terms of the final glass structural characteristics. It was found that testing the potentials in a systematic way of composition change that is wide enough is essential to provide valuable evaluations of the potentials. Composition dependent potential sets such as Du and Kieu potential were found to reproduce boron coordination change with composition in good agreement with experiments and the DBX model, with Du potential giving the best agreement. Bauchy potential was found to work well only for compositions with small R values. At higher R values beyond the plateau region, it showed an opposite trend of B N_4 as compared to experiments. Similar behaviors were observed in the fraction of NBO as a function of composition. For sodium boroaluminosilicate glasses, Kieu potential (with the later added Al_2O_3 parameters) and Du potential also provide better agreement of B N_4 as compared to with model based on NMR. For mechanical properties, all of the three potential sets were able to reproduce the trend with composition (R value) but they all tend to overestimate the elastic moduli. Overall, all the three potentials have some room of improvements: Du potential gives overall the best agreement of boron coordination and NBO with composition but it slightly overestimates the B-O distance; Kieu potential also works pretty well in both borosilicate and boroaluminosilicate glasses but it has the most fitting parameters with composition dependent charge and B-O interactions hence make it very difficult to expand. Bauchy potential on the other fails to provide the correct B coordination change for a wide range of compositions hence can only work in certain compositions although it has the simplest form with fixed parameters. Both the Du and Bauchy potentials have the possibility to model multicomponent glasses to build up existing

potential sets. Hence, the development of boron potential is not a finished business but instead needs further investment. It is believed that these recent active developments of boron potentials will enable further refining of existing and proposing of new empirical potentials to enable reliable simulations of borosilicate and other borate containing glasses.

Author Contributions

Manzila Tuheen: Methodology, Data curation, Formal analysis, Writing- original draft, Writing - review & editing. **Lu Deng:** Investigation, Formal analysis, Writing - original draft, Writing – review & editing. **Jincheng Du:** Conceptualization, Formal analysis, Funding acquisition, Supervision, Writing - original draft, Writing - review & editing.

Acknowledgement

This research has been made possible through support from the Center for Performance and Design of Nuclear Waste Forms and Containers, an Energy Frontier Research Center funded by the U.S. DOE, Office of Science, Basic Energy Sciences under Award No. DE-SC0016584 and U.S. National Science Foundation DMR Ceramics Program (#1508001). We would like thank Dr. Alfonso Pedone for helpful discussions. Computer support was provided by UNT's High Performance Computing Service.

References

[1] Q. Fu, M. N. Rahaman, H. Fu, and X. Liu, "Silicate, borosilicate, and borate bioactive glass scaffolds with controllable degradation rate for bone tissue engineering applications. I. Preparation and in vitro degradation," *J. Biomed. Mater. Res. - Part A*, vol. 95, no. 1, pp. 164–171, 2010.

[2] J. C. Phillips and R. Kerner, "Structure and function of window glass and Pyrex," *J. Chem. Phys.*, vol. 128, no. 17, 2008.

[3] M. M. Smedskjaer, R. E. Youngman, and J. C. Mauro, "Principles of Pyrex® glass chemistry: Structure-property relationships," *Appl. Phys. A Mater. Sci. Process.*, vol. 116, no. 2, pp. 491–504, 2014.

[4] M. M. Smedskjaer, J. C. Mauro, R. E. Youngman, C. L. Hogue, M. Potuzak, and Y. Yue, "Topological principles of borosilicate glass chemistry," *J. Phys. Chem. B*, vol. 115, no. 44, pp. 12930–12946, 2011.

[5] W. J. Weber *et al.*, "Waste and Plutonium Disposition," *J. Mater. Res.*, vol. 12, no. 8, pp. 1946–1978, 1997.

[6] J. D. Vienna, J. V. Ryan, S. Gin, and Y. Inagaki, "Current understanding and remaining challenges in modeling long-term degradation of borosilicate nuclear waste glasses," *Int. J. Appl. Glas. Sci.*,

vol. 4, no. 4, pp. 283–294, 2013.

[7] S. Gin *et al.*, “An international initiative on long-term behavior of high-level nuclear waste glass,” *Mater. Today*, vol. 16, no. 6, pp. 243–248, 2013.

[8] K. Raj and C. P. Kaushik, “Glass matrices for vitrification of radioactive waste - An update on R & D efforts,” *IOP Conf. Ser. Mater. Sci. Eng.*, vol. 2, 2009.

[9] M. I. Ojovan and O. G. Batyukhnova, “Glasses for Nuclear Waste Immobilization,” *WM ’07 Conf.*, no. November, p. 15, 2007.

[10] X. Lu *et al.*, “Mixed Network Former Effect on Structure, Physical Properties, and Bioactivity of 45S5 Bioactive Glasses: An Integrated Experimental and Molecular Dynamics Simulation Study,” *J. Phys. Chem. B*, vol. 122, no. 9, pp. 2564–2577, 2018.

[11] Y. D. Yiannopoulos, G. D. Chryssikos, and E. I. Kamitsos, “Structure and properties of alkaline earth borate glasses,” *Phys. Chem. Glas.*, vol. 42, no. 3, pp. 164–172, 2001.

[12] A. C. Wright, G. Dalba, F. Rocca, and N. M. Vedishcheva, “Borate versus silicate glasses: Why are they so different?,” *Phys. Chem. Glas. Eur. J. Glas. Sci. Technol. Part B*, vol. 51, no. 5, pp. 233–265, 2010.

[13] N. A. Ghoneim and A. F. Abbas, “Thermal expansion of high lead borate glasses and the boric oxide anomaly,” *Thermochim. Acta*, vol. 66, no. 1–3, pp. 91–103, 1983.

[14] W. J. Dell, P. J. Bray, and S. Z. Xiao, “11B NMR studies and structural modeling of Na2OB2O3SiO2 glasses of high soda content,” *J. Non. Cryst. Solids*, vol. 58, no. 1, pp. 1–16, 1983.

[15] O. Bouty, J. M. Delaye, and S. Peuget, “Europium Structural Effect on a Borosilicate Glass of Nuclear Interest,” *Procedia Chem.*, vol. 7, pp. 540–547, 2012.

[16] J. Wu, J. F. Stebbins, and T. Rouxel, “Cation Field Strength Effects on Boron Coordination in Binary Borate Glasses,” *J. Am. Ceram. Soc.*, vol. 97, no. 9, pp. 2794–2801, 2014.

[17] Y. H. Yun and P. J. Bray, “Nuclear magnetic resonance studies of the glasses in the system K2OB2O3P2O5,” *J. Non. Cryst. Solids*, vol. 30, no. 1, pp. 45–60, 1978.

[18] M. M. Smedskjaer, J. C. Mauro, S. Sen, and Y. Yue, “Quantitative design of glassy materials using temperature-dependent constraint theory,” *Chem. Mater.*, vol. 22, no. 18, pp. 5358–5365, 2010.

[19] L. S. Du and J. F. Stebbins, “Network connectivity in aluminoborosilicate glasses: A high-resolution 11B, 27Al and 17O NMR study,” *J. Non. Cryst. Solids*, vol. 351, no. 43–45, pp. 3508–3520, 2005.

[20] W. Soppe and H. W. den Hartog, “A molecular dynamics study of (B2O3)1-x-y(Li2O)x(Li2Cl2)y and (B2O3)1-x-y(Li2O)x(Cs2O)y,” *J. Non. Cryst. Solids*, vol. 108, no. 3, pp. 260–268, 1989.

[21] L.-H. Kieu, D. Kilymis, J.-M. Delaye, and S. Peuget, “Discussion on the Structural Origins of the Fracture Toughness and Hardness Changes in Rapidly Quenched Borosilicate Glasses: A Molecular Dynamics Study,” *Procedia Mater. Sci.*, vol. 7, pp. 262–271, 2014.

[22] H. Search, C. Journals, A. Contact, M. Iopscience, and I. P. Address, “Computer modelling of & Os : part I . New interatomic potentials , crystalline phases and predicted polymorphs,” vol. 8659, 1995.

[23] A. Takada *et al.*, "Related content Computer modelling of B 2 O 3 . II . Molecular dynamics simulations of vitreous structures Computer modelling of Bz03 : part 11 . Molecular dynamics simulations of vitreous structures," 1995.

[24] L. Huang and J. Kieffer, "Molecular dynamics study of cristobalite silica using a charge transfer three-body potential: Phase transformation and structural disorder," *J. Chem. Phys.*, vol. 118, no. 3, pp. 1487–1498, 2003.

[25] L. Huang and J. Kieffer, "Thermomechanical anomalies and polyamorphism in B2 O3 glass: A molecular dynamics simulation study," *Phys. Rev. B - Condens. Matter Mater. Phys.*, vol. 74, no. 22, pp. 1–10, 2006.

[26] H. Inoue, A. Masuno, and Y. Watanabe, "Modeling of the structure of sodium borosilicate glasses using pair potentials," *J. Phys. Chem. B*, vol. 116, no. 40, pp. 12325–12331, 2012.

[27] L. H. Kieu, J. M. Delaye, L. Cormier, and C. Stolz, "Development of empirical potentials for sodium borosilicate glass systems," *J. Non. Cryst. Solids*, vol. 357, no. 18, pp. 3313–3321, 2011.

[28] L. Deng and J. Du, "Development of effective empirical potentials for molecular dynamics simulations of the structures and properties of boroaluminosilicate glasses," *J. Non. Cryst. Solids*, vol. 453, pp. 177–194, 2016.

[29] L. Deng and J. Du, "Development of boron oxide potentials for computer simulations of multicomponent oxide glasses," *J. Am. Ceram. Soc.*, vol. 102, no. 5, pp. 2482–2505, 2019.

[30] M. Wang, N. M. Anoop Krishnan, B. Wang, M. M. Smedskjaer, J. C. Mauro, and M. Bauchy, "A new transferable interatomic potential for molecular dynamics simulations of borosilicate glasses," *J. Non. Cryst. Solids*, vol. 498, no. December 2017, pp. 294–304, 2018.

[31] B. Guillot and N. Sator, "A computer simulation study of natural silicate melts. Part II: High pressure properties," *Geochim. Cosmochim. Acta*, vol. 71, no. 18, pp. 4538–4556, 2007.

[32] B. Stevensson, Y. Yu, and M. Edén, "Structure-composition trends in multicomponent borosilicate-based glasses deduced from molecular dynamics simulations with improved B-O and P-O force fields," *Phys. Chem. Chem. Phys.*, vol. 20, no. 12, pp. 8192–8209, 2018.

[33] F. Pacaud, M. Salanne, T. Charpentier, and L. Cormier, "simulations using a polarizable force fi eld," *J. Non-Cryst. Solids*, vol. 499 , pp. 371–379, 2018.

[34] F. Pacaud, J. Delaye, T. Charpentier, and L. Cormier, "Structural study of Na 2 O – B 2 O 3 – SiO 2 glasses from molecular simulations using a polarizable force field," *J. Chem. Phys.* vol. 161711, no. June, 2017.

[35] M. Fortino *et al.*, "Assessment of interatomic parameters for the reproduction of borosilicate glass structures via DFT-GIPAW calculations," *J. Am. Ceram. Soc.*, vol. 102, no. 12, pp. 7225–7243, 2019.

[36] K. H. Lee, Y. Yang, B. Ziebarth, W. Mannstadt, M. J. Davis, and J. C. Mauro, "Evaluation of classical interatomic potentials for molecular dynamics simulations of borosilicate glasses," *J. Non. Cryst. Solids*, vol. 528, 2020.

[37] M. Bauchy, B. Guillot, M. Micoulaut, and N. Sator, "Viscosity and viscosity anomalies of model silicates and magmas: A numerical investigation," *Chem. Geol.*, vol. 346, pp. 47–56, 2013.

[38] R. Vuilleumier, N. Sator, and B. Guillot, "Computer modeling of natural silicate melts: What can we learn from ab initio simulations," *Geochim. Cosmochim. Acta*, vol. 73, no. 20, pp. 6313–6339,

2009.

[39] L. Du and J. F. Stebbins, “Network connectivity in aluminoborosilicate glasses :,” vol. 351, pp. 3508–3520, 2005.

[40] J. Du and A. N. Cormack, “Erratum: ‘The medium range structure of sodium silicate glasses: A molecular dynamics simulation’ by J. Du and A.N. Cormack (Journal of Non-Crystalline Solids (2004) 349 (66-79) DOI:10.1016/j.jnoncrysol.2004.08.264),” *J. Non. Cryst. Solids*, vol. 351, no. 10–11, p. 956, 2005.

[41] J. Du and A. N. Cormack, “The medium range structure of sodium silicate glasses: A molecular dynamics simulation,” *J. Non. Cryst. Solids*, vol. 349, no. 1–3, pp. 66–79, 2004.

[42] M. Collin *et al.*, “The structure of ISG glass and the properties of its passivating layer formed in neutral pH conditions,” *npj Mat. Deg.*, vol. 2, p. 4, 2018.

[43] X. Lu, M. Ren, L. Deng, C. J. Benmore, and J. Du, “Structural features of ISG borosilicate nuclear waste glasses revealed from high-energy X-ray diffraction and molecular dynamics simulations,” *J. Nucl. Mater.*, vol. 515, pp. 284–293, 2019.

[44] M. Ren, X. Lu, L. Deng, P. H. Kuo, and J. Du, “B2O3/SiO2substitution effect on structure and properties of Na2O-CaO-SrO-P2O5-SiO2bioactive glasses from molecular dynamics simulations,” *Phys. Chem. Chem. Phys.*, vol. 20, no. 20, pp. 14090–14104, 2018.

[45] X. Lu *et al.*, “Mixed Network Former Effect on Structure, Physical Properties, and Bioactivity of 45S5 Bioactive Glasses: An Integrated Experimental and Molecular Dynamics Simulation Study,” *J. Phys. Chem. B*, vol. 122, no. 9, 2018.

[46] X. Lu, L. Deng, P.-H. Kuo, M. Ren, I. Buterbaugh, and J. du, “Effects of boron oxide substitution on the structure and bioactivity of SrO-containing bioactive glasses,” *J. Mater. Sci.*, 2017.

[47] I. Todorov, W. Smith, and U. Cheshire, “The DL POLY 4 user manual,” *STFC, STFC Daresbury …*, no. January, 2011.

[48] A. Pedone, “Properties Calculations of Silica-Based Glasses by Atomistic Simulations Techniques : A Review,” pp. 20773–20784, 2009.

[49] L. Deng and J. Du, “Effects of system size and cooling rate on the structure and properties of sodium borosilicate glasses from molecular dynamics simulations,” *J. Chem. Phys.*, vol. 148, no. 2, 2018.

[50] M. Ren, L. Deng, and J. Du, “Bulk, surface structures and properties of sodium borosilicate and boroaluminosilicate nuclear waste glasses from molecular dynamics simulations,” *J. Non. Cryst. Solids*, vol. 476, no. May, pp. 87–94, 2017.

[51] S. Plimpton, “LAMMPS documentation,” *… . cs. sandia. gov/~ sjplimp/lammps/doc/Manual. html*, 2007.

[52] J. Du, C. J. Benmore, R. Corrales, R. T. Hart, and J. K. R. Weber, “A molecular dynamics simulation interpretation of neutron and x-ray diffraction measurements on single phase Y(2)O(3)-Al(2)O(3) glasses.,” *J. Phys. Condens. Matter*, vol. 21, no. 20, p. 205102, 2009.

[53] D. I. Grimley, A. C. Wright, and R. N. Sinclair, “Neutron scattering from vitreous silica IV. Time-of-flight diffraction,” *J. Non. Cryst. Solids*, vol. 119, no. 1, pp. 49–64, 1990.

[54] A. F. P. L. D. R. & S. J. G. G. N. Greaves*, “Local structure of silicate glasses,” *Nature*, vol. 293, no. October, pp. 611–616, 1981.

[55] M. Fábián, P. Jóvári, E. Sváb, G. Mészáros, T. Proffen, and E. Veress, “Network structure of 0.7SiO2-0.3Na2O glass from neutron and x-ray diffraction and RMC modelling,” *J. Phys. Condens. Matter*, vol. 19, no. 33, pp. 0–11, 2007.

[56] O. Majérus, L. Cormier, G. Calas, and B. Beuneu, “Temperature-induced boron coordination change in alkali borate glasses and melts,” *Phys. Rev. B - Condens. Matter Mater. Phys.*, vol. 67, no. 2, pp. 1–7, 2003.

[57] R. L. Mozzi and B. E. Warren, “The structure of vitreous boron oxide,” *J. Appl. Crystallogr.*, vol. 3, no. 4, pp. 251–257, 1970.

[58] L. Pedesseau, S. Ispas, and W. Kob, “First-principles study of a sodium borosilicate glass-former. I. the liquid state,” *Phys. Rev. B - Condens. Matter Mater. Phys.*, vol. 91, no. 13, pp. 1–14, 2015.

[59] J. F. Stebbins, “Cation sites in mixed-alkali oxide glasses: Correlations of NMR chemical shift data with site size and bond distance,” *Solid State Ionics*, vol. 112, no. 1–2, pp. 137–141, 1998.

[60] X. Yuan and A. N. Cormack, “Efficient algorithm for primitive ring statistics in topological networks,” *Comput. Mater. Sci.*, vol. 24, no. 3, pp. 343–360, 2002.

[61] R. Hill, “The elastic behaviour of a crystalline aggregate,” *Proc. Phys. Soc. Sect. A*, vol. 65, no. 5, pp. 349–354, 1952.

[62] S. Plimpton, “Fast parallel algorithms for short-range molecular dynamics,” *Journal of Computational Physics*, vol. 117, no. 1. pp. 1–19, 1995.

[63] R. Takahashi, K; Osaka, A; Furuno, “The elastic properties of the glasses in the system R2O-B2O3-SiO2 (R= Na and K) and Na2O-B2O3,” *J ceram Assoc Japan*, vol. 91, pp. 199–215, 1983.

[64] D. M. Zirl and S. H. Garofalini, “Structure of Sodium Aluminosilicate Glasses,” *J. Am. Ceram. Soc.*, vol. 73, no. 10, pp. 2848–2856, 1990.

[65] D. A. McKeown, G. A. Waychunas, and G. E. Brown, “Exafs and xanes study of the local coordination environment of sodium in a series of silica-rich glasses and selected minerals within the Na2OAl2O3SiO2 system,” *J. Non. Cryst. Solids*, vol. 74, no. 2–3, pp. 325–348, 1985.

[66] F. G, “Issledovanie Alyumo-Bornoi Anomalii Svoistv Silikatnykh Stekol,” 1959.

[67] S. Sundararaman, L. Huang, S. Ispas, and W. Kob, “New interaction potentials for borate glasses with mixed network formers,” pp. 1–22.